Hindawi
Wireless Communications and Mobile Computing
Volume 2021, Article ID 6622168, 12 pages
https://doi.org/10.1155/2021/6622168

Research Article

Research on Pattern Synthesis of Time Modulated Sparse Array Based on Discrete Variable Convex Optimization

Jing Tan[1,2] **Jiawen Hu**[1] **Xikuan Dong**[1] **Hailin Li**[1] **and Jianjiang Zhou**[1]

[1]*College of Electronic and Information Engineering, Nanjing University of Aeronautics and Astronautics, No. 29 Jiangjun Avenue, 210016 Nanjing, China*
[2]*Nanhang Jincheng College, No. 88, Hangjin Road, Lukou Street, Jiangning, 211156 Nanjing, China*

Correspondence should be addressed to Jiawen Hu; nuaahjw@nuaa.edu.cn

Received 15 December 2020; Revised 13 January 2021; Accepted 26 March 2021; Published 9 April 2021

Academic Editor: Zhipeng Cai

Effective resource utilization is an important problem in the application of array, especially for the new time modulated array. Considering the problem of full utilization of array elements in time modulated array, a sparse optimization algorithm based on discrete variable convex optimization is proposed in this paper. The pattern optimization of equal excitation time modulation array is realized in two stages: In the first stage, the number of working array elements is as low as possible under the condition of suppressing the sidelobe of the central frequency. In the second stage, the sideband is suppressed by iterative convex optimization. The numerical simulation results are compared with other methods to verify the effectiveness of the proposed method in pattern optimization of equal excitation time modulation array. Finally, the optimization performance of the algorithm with different array parameters is verified.

1. Introduction

Using Radio Frequency (RF) switch to control the working state of each antenna channel, time modulated technology can change the pattern parameters of phased array antenna [1], which has been widely used in satellite communication, radar, and other fields. Compared with the ordinary array, time modulated array can meet the requirements of engineering practice for high performance of antenna array [2]. Therefore, more and more researchers have done deep research on time modulated array in recent years.

However, due to the introduction of RF switches, time modulated array needs more complex design in the hardware system. In order to achieve higher performance and meet the technical requirements of practical engineering. Some researches have improved the hardware system of time modulated array: The digital attenuator is used to generate S-step waveform to expand the signal bandwidth and reduce the radiation loss in [3]. The multibranch time modulated model is used to replace the phase shifter and attenuator to expand the beam scanning range and improve the scanning accuracy in [4]. A reconfigurable power divider is proposed to ensure the instantaneous gain stability of the time modulated array in [5]. In order to improve the performance of time modulated array, some new sequential switches have been proposed: A new type of switch is proposed to improve the feed efficiency of time modulated antenna array in [6]. A new method to improve the gain of time modulated antenna array by using single pole double throw switch is proposed in [7]. An improved phase modulated technique based on four-dimensional antenna array is proposed in [8], which improved control unit consists of two single pole double throw switches and four different delay lines and realize beam control and beamforming at any angle. The above research effectively improves the performance of the time modulated array through the improvement of the hardware system. But both consider the optimization of the RF switch and the power division network, which makes the system design more complex. Compared with the ordinary time modulated array, the equal excitation time modulated array controls the amplitude and phase of static excitation to a fixed value, reduces the hardware modules such as power

attenuator and phase shifter, and effectively reduces the complexity of the hardware system. Some scholars have applied the optimization algorithm to the equal excitation time modulated array: The sidelobe optimization problem in the equal excitation time modulated array is studied in [9]. A new technique of synthesizing equidistant linear array with equal excitation time modulated array by firefly algorithm is proposed in [10]. [11] used the firefly algorithm (FA) algorithm to design the antenna unit of the equal excitation time modulated array, which is produced in the main frequency and the first sideband, respectively. A differential-based evolutionary algorithm (DE) is used to suppress the sidelobe and sideband of the equal excitation time modulated array in [12]. [13] proposed a new technology for synthesizing the equal excitation time modulated linear array by using the improved invasive weed optimization algorithm; [14] used the artificial bee colony algorithm to suppress the sidelobe and sideband of the equal excitation time modulated array.

The equal excitation time modulated array can effectively save the cost of the system level. The array sparse can reduce the number of working array elements, improve the utilization rate of antenna array elements, and reduce unnecessary loss under the condition of certain array aperture. There are a lot of sparse optimization for ordinary arrays: The synthesis method based on the matrix pencil method (MPM) and the forward-backward MPM (FBMPM) is extended in [15] to the synthesis of multimode linear array with fewer elements. A design method of sparse multimode linear array based on the enhanced unitary matrix pencil (EUMP) method is proposed in [16], which significantly reduces the computational complexity of array sparse optimization engineering. A new pattern reconfigurable sparse array synthesis technology is proposed in [17], which can be used between the number of active antenna elements and the pattern characteristics to achieve a reasonable compromise. An alternating convex optimization method is proposed in [18] to synthesize the single beam pattern sparse linear array. Although there are a lot of researches on sparse optimization methods for ordinary arrays, there are few studies on sparse time modulated arrays. The combination of equal excitation time modulated arrays and array sparsity is an important method to simplify array structure and save cost. How to reduce the number of working array elements as much as possible of the equal excitation time array is a topic worth exploring.

The method proposed in this paper grasps the discrete characteristic that the working state of the time modulated array. Using discrete variable convex optimization method to realize the sparse optimization of the equal excitation time modulated array and effectively suppress the sidelobe level of the main frequency and sideband level. Compared with the other array sparseness method, the proposed method greatly reduces the time of sparse optimization process by using the convex characteristics of the array elements. At the same time, the method proposed in this paper selects the working elements from a certain number of equal excitation time modulation full array, which is easier to realize in practice.

The structure of this paper is as follows: The mathematical models of sparse optimization, sidelobe optimization, and sideband optimization of equal excitation time array is introduced in Section 2. Section 3 introduces how to use discrete variable convex optimization algorithm to achieve sparse optimization of array and sidelobe suppression of main frequency and use iterative convex optimization method to achieve sideband suppression. In Section 4, the numerical simulation results are compared with other methods to verify the effectiveness of the algorithm in the sparse optimization and sidelobe and sideband suppression of the equal excitation time modulation array and explore the influence of array parameters on the optimization results. Finally, it is summarized in Section 5.

2. Mathematical Model

As shown in Figure 1, the far-field radiation intensity based on equal excitation time modulated linear array is

$$E(\theta, t) = \sum_n u_n(t) e^{jkx_n(\sin\theta - \sin\theta_0)} e^{j2\pi f_0 t}, \tag{1}$$

where θ_0 is the main radiation direction, f_0 is the central frequency, $k = 2\pi f_0 c$, c is the light speed, x_n is the position of the nth elements, and $u_n(t)$is the function of RF switch (for more explanations of the symbols in this paper, see Table 1).

As shown in Figure 2, T_r is the time modulation repetition period of RF switch;$u_n(t)$ is a rectangular function, and its mathematical expression is

$$u_n(t) = \varepsilon(t - t_n) - \varepsilon(t - t_n - \tau_n), \tag{2}$$

where $\varepsilon(t)$ is the step function, t_n is the switch-ON time instant, and τ_n is the switch-ON duration time, $0 \le t_n, \tau_n \le T_r$; expanding $u_n(t)$ by Fourier transform

$$u_n(t) = \sum_m a_{nm} e^{j2\pi m f_r t}, m = 0, \pm 1, \cdots, \tag{3}$$

where $f_r = 1/T_r$ and a_{nm} is the expansion coefficient, and its expression is

$$a_{nm} = \tau_n f_{\mathrm{r}} \sin c(\pi m \tau_n f_r) e^{-j\pi m f_r (2t_n + \tau_n)}. \tag{4}$$

Equation (1) can be further expressed as

$$E(\theta, t) = \sum_n \sum_m a_{nm} e^{jkx_n(\sin\theta - \sin\theta_0)} e^{j2\pi(f_0 + mf_r)t}. \tag{5}$$

For the convenience of discussion, ignoring the common factor $e^{j2\pi(f_0+mf_r)t}$ and assuming $\alpha_n = \tau_n f_r$ and $\beta_n = t_n f_r$, the far-field radiation intensity of array antenna in mth sideband $f_0 + mf_r$ is

$$E_m(\theta) = \sum_n \alpha_n \sin c(\pi m \alpha_n) e^{jkx_n(\sin\theta - \sin\theta_0) - j\pi m(2\beta_n + \alpha_n)}. \tag{6}$$

Compared with ordinary array, the equal excitation time modulated linear array does not need power attenuator and phase shifter, which reduces the hardware cost. However,

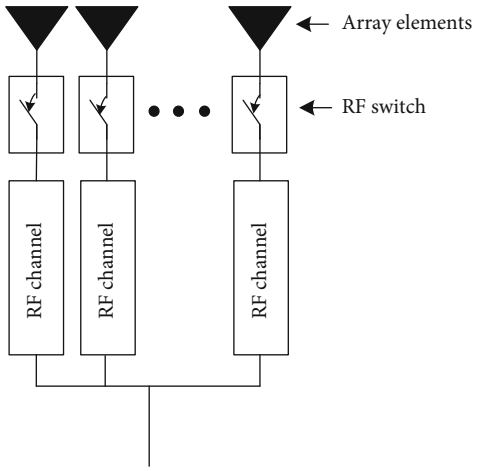

Figure 1: Basic structure for equal excitation time modulated array.

Table 1: The explanation of some symbols in this paper.

Name of symbols	Explanation of symbols
$u_n(t)$	The function of time sequence switch
T_r	The period of time sequence switch
t_n	The switch-ON time instant of time sequence switch
τ_n	The switch-ON duration time of time sequence switch
$\|\bullet\|_0$	The number of zero elements in a matrix
γ	Optimal sparse control coefficient
λ_n	Contrast parameter, the threshold to judge whether an element can be approximated to zero
μ	The ratio of the number of working array elements to the total number of arrays

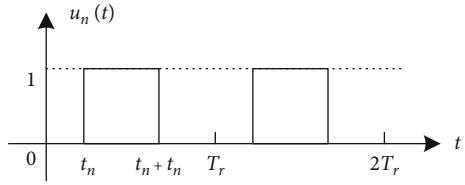

Figure 2: The function of time sequence switch.

time modulated technology brings the sideband effect of radiation, which needs to be suppressed. On the other hand, the hardware cost can be reduced by reducing the number of working elements. Based on the above requirements, the following pattern synthesis problems for the equal excitation time modulated linear array are studied:

(1) Suppress the sidelobe radiation intensity when the central frequency main lobe radiation intensity is given

(2) Minimizing the number of working array elements by sparse optimization

(3) Suppressing the sidebands when the central frequency radiation parameters are satisfied radiation intensity

The constraints on the main frequency band and sideband are shown in Figure 3, where the red line represents the central frequency pattern and the blue line represents the sideband pattern. θ_0 is the radiation direction on the central frequency. Ω_s is the sidelobe region on the central frequency. ε_1 and ε_2 are the sidelobe and sideband constraint parameters. It can be expressed as the following combinatorial optimization problem model

$$\begin{aligned} (\mathrm{P1}) \quad & \min_{\boldsymbol{\alpha},\boldsymbol{\beta}} \quad \|\boldsymbol{\alpha}\|_0 \\ & \text{s.t.} \quad E_0(\theta_s) \le \varepsilon_1 * E_0(\theta_0), \theta_s \in \Omega_s \\ & \qquad E_m(\theta_i) \le \varepsilon_2 * E_0(\theta_0), \theta_i \in \Omega_m \\ & \qquad 0 \le \alpha_n, \beta_n \le 1, \end{aligned} \tag{7}$$

where $\boldsymbol{\alpha} = [\alpha_1 \cdots \alpha_N]^T$ and $\boldsymbol{\beta} = [\beta_1 \quad \cdots \quad \beta_N]^T$ are the parameter vectors to be optimized. $\|\boldsymbol{\alpha}\|_0$ is the 0 norm of the vector, which is the number of array elements whose working time is greater than 0. $E_0(\theta_0)$ is the radiation intensity at the radiation direction θ_0 on the central frequency. $E_0(\theta_s), s = 1, 2 \cdots$ is the radiation intensity at the sampling direction θ_s of the sidelobe region Ω_s on the central frequency. $E_m(\theta_i), i = 1, 2 \cdots$ is the sampling direction θ_i of the radiation area Ω_m on the mth sideband. ε_1 and ε_2 are the sidelobe and sideband constraint parameters.

3. Proposed Algorithm

Further analyse the expression of formula (6), when $m = 0$, $E_0(\theta) = \sum_n \alpha_n e^{jkx_n \sin\theta}$is only related to α_n.The pattern on the central frequency is only related to the switch-ON duration time and is independent of the turn on time t_n. When $m \neq 0$, $\sin c(\pi m \alpha_n)$ is included by $E_m(\theta)$. With the increase of m, each summation item becomes smaller, which makes each sideband less than central frequency.

Based on the above analysis, we decompose the combinatorial optimization problem represented by equation (7) into two optimization problems

(1) Solve the optimal the switch-ON duration time τ_n to satisfy the constraints of sidelobe on the central frequency, where γ is the sparse control coefficient

$$\begin{aligned} (\mathrm{P2}) \quad & \min_{\boldsymbol{\alpha}} \quad E_0(\theta_0) + \gamma\|\boldsymbol{\alpha}\|_0 \\ & \text{s.t.} \quad 0 \le \alpha_n \le 1 \\ & \qquad E_0(\theta_s) \le \varepsilon_1 * E_0(\theta_0), \theta_s \in \Omega_s. \end{aligned} \tag{8}$$

(2) On the basis of solving problem P2, given the switch-ON duration time τ_n of each element, solve switch-

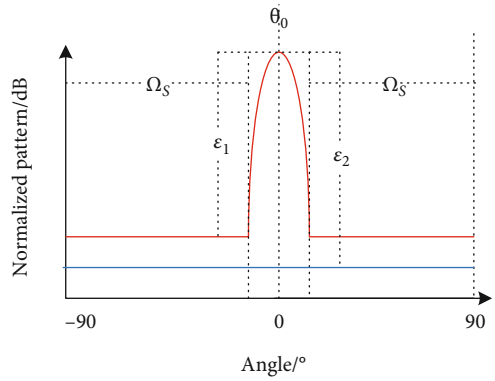

Figure 3: Constraint pattern.

ON time instant t_n to satisfy the constraints of each order of sidebands

$$\begin{aligned}(\text{P3})\quad &\min_{\boldsymbol{\beta}} \quad \varepsilon_2 \\ &\text{s.t.} \quad 0 \le \beta_n \le 1 \\ &\qquad E_m(\theta_i) \le \varepsilon_2 * E_0(\theta_0), \theta_i \in \Omega_m.\end{aligned} \tag{9}$$

3.1. Problem Solving of P2. $\|\boldsymbol{\alpha}\|_0$ is the number of nonzero elements in vector $\boldsymbol{\alpha}$, which is also called the cardinality of vector $\boldsymbol{\alpha}$. Therefore, the optimization problem of equation (8) is a nonconvex problem. In this paper, a sequential convex approximation method is proposed to solve the sparse optimization problem. By constructing the approximation function of $\|\boldsymbol{\alpha}\|_0$ term and linearizing the concave part of the approximation function, a series of convex subproblems are obtained. The optimal solutions of these subproblems approximate the optimal solution of problem P2. A binary variable $\delta_n \in \{0, 1\}$ is introduced to indicate whether α_n is zero or not; then, equation (8) is equivalent to mixed integer programming

$$\begin{aligned}(\text{P4})\quad &\min_{\boldsymbol{\alpha}} \quad E_0(\theta_0) + \gamma \sum_n \delta_n \\ &\text{s.t.} \quad \delta_n \in \{0, 1\} \\ &\qquad 0 \le \alpha_n \le 1 \\ &\qquad \alpha_n(1 - \delta_n) = 0 \\ &\qquad E_0(\theta_s) \le \varepsilon_1 * E_0(\theta_0), \theta_s \in \Omega_s.\end{aligned} \tag{10}$$

Construct the approximate function $g(\boldsymbol{\alpha}) = \sum_n \delta_n + \sum_n \lambda_n \alpha_n (1 - \delta_n)$ of $\|\boldsymbol{\alpha}\|_0$, where $\boldsymbol{\lambda} = [\lambda_1 \quad \cdots \quad \lambda_N]^T, \forall n, \lambda_n \ge 1$ is the comparison parameter. Then, equation (10) is equivalent to solving the optimization problem

$$\begin{aligned}(\text{P5})\quad &\min_{\boldsymbol{\alpha}} \quad E_0(\theta_0) + \gamma g(\boldsymbol{\alpha}) \\ &\text{s.t.} \quad \delta_n \in \{0, 1\} \\ &\qquad 0 \le \alpha_n \le 1 \\ &\qquad E_0(\theta_s) \le \varepsilon_1 * E_0(\theta_0), \theta_s \in \Omega_s,\end{aligned} \tag{11}$$

where $\delta_n + \lambda_n \alpha_n (1 - \delta_n) = \begin{cases} \lambda_n \alpha_n & \delta_n = 0 \\ 1 & \delta_n = 1 \end{cases}$, so $\min\{\delta_n + \lambda_n \alpha_n (1 - \delta_n)\}$ is equal to $\min\{\lambda_n \alpha_n, 1\}$. And there is

$$\delta_n + \lambda_n \alpha_n (1 - \delta_n) = \begin{cases} \lambda_n \alpha_n & 0 \le \alpha_n < \lambda_n^{-1} \\ 1 & \lambda_n^{-1} \le \alpha_n \le 1 \end{cases}. \tag{12}$$

Equation (12) is a nonnegative piecewise linear concave function on interval $0 \le \alpha_n \le 1$. So we can decompose $g(\boldsymbol{\alpha})$ into the difference between two convex functions

$$g(\boldsymbol{\alpha}) = c_1(\boldsymbol{\alpha}) - c_2(\boldsymbol{\alpha}), \tag{13}$$

where $c_1(\boldsymbol{\alpha}) = \sum_n \lambda_n \alpha_n$ and $c_2(\boldsymbol{\alpha}) = \sum_n \lambda_n \max\{0, \alpha_n - \lambda_n^{-1}\}$ are the two convex functions. Since $-c_2(\boldsymbol{\alpha})$ is a concave function, $-c_2(\boldsymbol{\alpha})$ can be linearized by sequence

$$c_2(\boldsymbol{\alpha}) = c_2\left(\boldsymbol{\alpha}^{(k)}\right) + \boldsymbol{\eta}^{T(k)}\left(\boldsymbol{\alpha} - \boldsymbol{\alpha}^{(k)}\right), \tag{14}$$

where $\boldsymbol{\eta}^{(k)} = \partial c_2(\boldsymbol{\alpha}^{(k)})$ is the gradient of $c_2(\boldsymbol{\alpha})$ at $\boldsymbol{\alpha}^{(k)}$; its components are

$$\eta_n^{(k)} = \begin{cases} 0 & 0 \le \alpha_n^{(k)} < \lambda_n^{-1} \\ \lambda_n & \lambda_n^{-1} \le \alpha_n^{(k)} \le 1 \end{cases}. \tag{15}$$

So the optimization subproblem of degree $k + 1$ is

$$\begin{aligned}(\text{P6})\quad &\min_{\boldsymbol{\alpha}} \quad E_0(\theta_0) + \gamma h(\boldsymbol{\alpha}) \\ &\text{s.t.} \quad 0 \le \alpha_n \le 1 \\ &\qquad E_0(\theta_s) \le \varepsilon_1 * E_0(\theta_0), \theta_s \in \Omega_s,\end{aligned} \tag{16}$$

where $h(\boldsymbol{\alpha}) = c_1(\boldsymbol{\alpha}) - c_2(\boldsymbol{\alpha}^{(k)}) - \boldsymbol{\eta}^{T(k)}(\boldsymbol{\alpha} - \boldsymbol{\alpha}^{(k)})$ is a linear function about $\boldsymbol{\alpha}$.

Note that the steering vector at the radiation direction θ_0 of the main lobe of the array is $\mathbf{b}_0 = [1 \quad \cdots \quad 1]^T$. And that at the sampling direction θ_s of the sidelobe region is $\mathbf{b}_s = \left[e^{jkx_1(\sin\theta_s - \sin\theta_0)} \quad \cdots \quad e^{jkx_N(\sin\theta_s - \sin\theta_0)}\right]^T$. The optimization subproblem of equation (16) is further expressed as

$$\begin{aligned}(\text{P7})\quad &\min_{\boldsymbol{\alpha}} \quad \boldsymbol{\alpha}^T \mathbf{b}_0 + \gamma h(\boldsymbol{\alpha}) \\ &s.t. \quad 0 \le \alpha_n \le 1 \\ &\qquad \left\|\boldsymbol{\alpha}^T \mathbf{b}_s\right\| \le \varepsilon_1 * \boldsymbol{\alpha}^T \mathbf{b}_0, \theta_s \in \Omega_s.\end{aligned} \tag{17}$$

This is a quadratic constrained linear programming (QCLP) problem. The interior point method can be used to obtain the optimal solution $\boldsymbol{\alpha}^{(k+1)}$. The initial parameter $\boldsymbol{\alpha}^{(0)}$ of

sequential convex optimization can be solved by optimization of the minimum sidelobe of the full array (P8).

$$\begin{aligned}(\text{P8}) \quad \min_{\boldsymbol{\alpha}} \quad & \boldsymbol{\alpha}^T \mathbf{b}_0 \\ \text{s.t.} \quad & 0 \le \alpha_n \le 1 \\ & \left\| \boldsymbol{\alpha}^T \mathbf{b}_s \right\| \le \varepsilon_1 * \boldsymbol{\alpha}^T \mathbf{b}_0, \theta_s \in \Omega_s.\end{aligned} \tag{18}$$

3.2. Problem Solving of P3. Problem P2 has solved the value of $\boldsymbol{\alpha}$, the switch-ON duration time τ_n of each element. Problem P3 needs to solve the switch-ON time instant t_n of each element according to each sideband constraint, the parameter β_n in the solution (6).

When the depression angle θ is known, $\rho_{nm}(\theta) = \alpha_n \sin c(\pi m \alpha_n) e^{jkx_n(\sin\theta - \sin\theta_0) - j\pi m\alpha_n}$ is a constant parameter and since the parameter β_n to be optimized is exponential. Equation (6) is a nonconvex function. The short form (6) is

$$E_m(\theta) = \sum_n \rho_{nm}(\theta) e^{-j2\pi m\beta_n}. \tag{19}$$

Refer to [19], this problem can be solved by the sequential convex method of Taylor series linear expansion. Let $\beta_n = \beta_n^{(k)} + \mu_n$, where $\forall n, |\mu_n| \le \mu_0$, μ_0 denote a small positive number. From the first order Taylor approximation of the complex exponential function, there are

$$e^{-j2\pi m\beta_n} = (1 - j2\pi m\mu_n) e^{-j2\pi m\beta_n^{(k)}}. \tag{20}$$

Thus, equation (19) is transformed into

$$E_m(\theta, \boldsymbol{\mu}) = \sum_n (1 - j2\pi m\mu_n) \rho_{nm}(\theta) e^{-j2\pi m\beta_n^{(k)}}, \tag{21}$$

where $\boldsymbol{\mu} = [\mu_1 \quad \cdots \quad \mu_N]^T$ is an increment vector. Problem P3 is rewritten as a sequential convex optimization model for solving the optimal incremental vector $\boldsymbol{\mu}$.

$$\begin{aligned}(\text{P9}) \quad \min_{\boldsymbol{\mu}} \quad & \varepsilon_2 \\ \text{s.t.} \quad & \left\| (1 - j2\pi m\boldsymbol{\mu})^T \mathbf{b}_{im}^{(k)} \right\| \le \varepsilon_2 * \boldsymbol{\alpha}^T \mathbf{b}_0 \\ & 0 \le \mu_n \le \mu_0, \forall n,\end{aligned} \tag{22}$$

where $\mathbf{b}_{im}^{(k)} = \left[\rho_{1m}(\theta) e^{-j2\pi m\beta_1^{(k)}} \quad \cdots \quad \rho_{Nm}(\theta) e^{-j2\pi m\beta_N^{(k)}} \right]^T$ is a complex constant vector; therefore, problem P9 is also a quadratic constrained linear programming (QCLP) problem, and the interior point method can be used to obtain the optimal solution.

3.3. Algorithm Flow. The processing flow of the whole algorithm is given below, and the flow chart is shown in Figure 4.

(1) *Array Parameter Initialization.* the number of array element$N$, position x_n, central frequencyf_0, radiation directionθ_0, sidelobe area sampling direction θ_s and constraint parameter ε_1, and sideband region sampling direction θ_i

(2) According to equation (18), the central band guide vectors of problem P2 are $\mathbf{b}_0$ and $\mathbf{b}_s$, and the initial parameter $\boldsymbol{\alpha}^{(0)}$ and its gradient $\boldsymbol{\eta}^{(0)}$ and compare parameter $\boldsymbol{\lambda}$

(3) Solving the QCLP subproblem of equation (17) to obtain the optimal $\boldsymbol{\alpha}^{(k+1)}$of $k+1$-th step. Updating $\boldsymbol{\eta}^{(k+1)}$ according to equation (15)

(4) If $|\boldsymbol{\alpha}^{(k+1)} - \boldsymbol{\alpha}^{(k)}| \ge \varepsilon_0$, ε_0 is the minimum difference, return to (3) and continue iteration; otherwise, go to the next step

(5) Initialize $\beta_n^{(0)}$, μ_0, and calculate $\mathbf{b}_{im}^{(0)}$ according to equation (23)

(6) Solve the QCLP subproblem of equation (22), obtain the optimal $\boldsymbol{\mu}^{(k+1)}$ in the $k+1$-th step, update $\beta_n^{(k+1)}$ according to $\beta_n^{(k+1)} = \beta_n^{(k)} + \mu_n^{(k+1)}$, and update $\mathbf{b}_{im}^{(k+1)}$ according to equation (23)

(7) If $|\boldsymbol{\mu}^{(k+1)} - \boldsymbol{\mu}^{(k)}| \ge \varepsilon_0$, go back to (6) to continue iteration; otherwise, go to the next step

(8) According to the optimal $\boldsymbol{\alpha}^{(k+1)}$ and $\boldsymbol{\beta}^{(k+1)}$, calculate and output each order pattern of the array

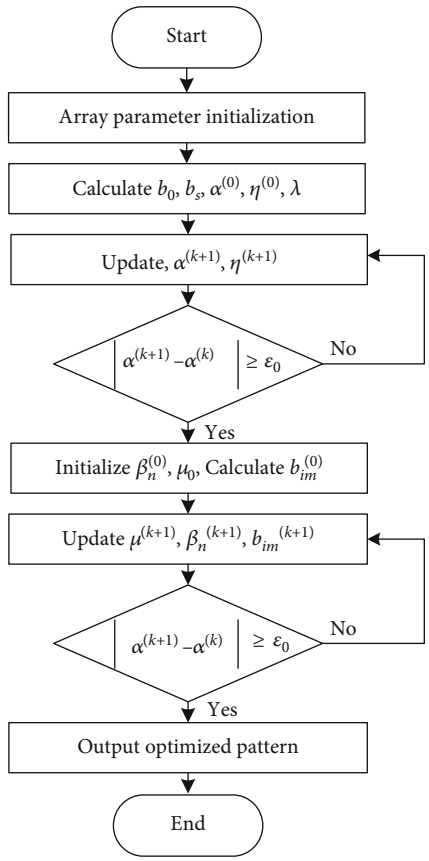

Figure 4: Algorithm flow chart.

4. Simulation Results

Compared with ordinary time modulated array, the power attenuator, phase shifter, and other hardware modules are reduced in the equal excitation time modulated linear array in order to reduce the hardware cost. In other words, in the process of pattern synthesis, the excitation amplitude and phase of the array element are fixed values, which could not be used as optimization parameters to improve the radiation performance of the array antenna. Due to this reason, the radiation pattern performance of the equal excitation time array will decrease compared with the ordinary time modulated array.

In order to evaluate the radiation performance of the equal excitation time array, pattern synthesis method based on convex optimization of discrete variable sequence is proposed in this paper, and three kinds of simulation experiments are designed to verify the effectiveness of the proposed algorithm:

(1) Pattern synthesis based on convex optimization of discrete variable sequences and sidelobe and sideband optimization of equal excitation time array

(2) Analysis of the influence of array parameters on the proposed method

(3) Sparse optimization of equal excitation time array

4.1. Pattern Synthesis Based on Sequence Convex Optimization and Sidelobe and Sideband Optimization of Equal Excitation Time Array. This part, sparsity is not considered. The sparse control coefficient $\gamma = 0$. The simulation is set to verify the effectiveness of the proposed method in pattern optimization of the equal excitation time modulated linear array.

In order to compare the optimization results with the PSO algorithm used in [20] and the HIWO algorithm used in [21], a 30 elements equal excitation time modulation line array is considered. The array parameters and pattern parameters are set as shown in Table 2.

Using the method proposed in this paper, the pattern is obtained in a short time of 2.15 s. The effect of the pattern on the main frequency band and the first to fifth sidebands is shown in Figure 5. It can be seen that the sidelobe level (SLL) of the main frequency band after optimization is -25 dB, and the maximum level ($SBL1 \sim 5$) of each sideband is -26.9 dB, -33.6 dB, -34.8 dB, -38.9 dB, and -36.7 dB, respectively.

The results show that:

(1) The sidelobe and sideband constraints reach the specified level ($SLL \leq -25dB$, $SBL \leq -25dB$) after using the proposed algorithm

(2) The maximum electric average of the optimized sideband is less than the first and second sideband levels, so only the first two sidebands can be constrained in formula (22)

In order to verify the effectiveness of the algorithm, we compare the results of PSO algorithm in reference [20] and HIWO algorithm in reference [21] under the same simulation conditions, as shown in Table 3.

Table 2: Array parameter.

Parameter name	Parameter value
N	30
d	0.7λ
Angle sampling interval	0.1°
θ_0	0°
$FNBW$	12°

Where N is the number of array elements, d is the interval between adjacent elements, θ_0 is the radiation direction of the main frequency band, and FNBW is the main lobe width of the main frequency band. The sidelobe and sideband optimization performance of equal excitation time modulation array is analysed under the condition of $\gamma = 0$.

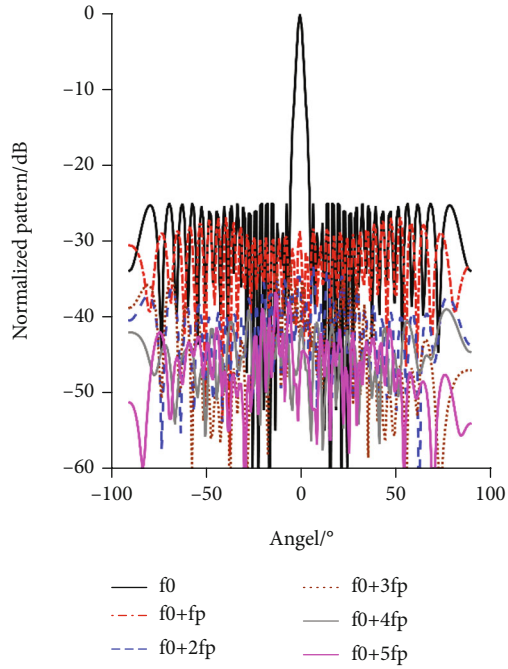

Figure 5: Optimized pattern at the central frequency and at front five sidebands of time modulated array.

From the results in Table 3, we can see that (1) the optimization time of the proposed algorithm is much less than that of PSO and HIWO algorithms, (2) the performance of the proposed algorithm is equivalent to that of the reference [21] algorithm and better than that of the reference [20] algorithm, and (3) the SBL1 and SBL2 of the proposed algorithm are slightly higher than those of the PSO and the HIWO algorithm.

The algorithm in references [20, 21] adds the degree of freedom of excitation, but the method proposed in this paper is applied to the equal excitation time modulated array. In order to simplify the complexity and cost of the hardware system, the power divider and phase shifter are removed, so the performance of the algorithm in this paper is slightly poor. However, the sideband levels are all lower than -25 dB, which meets the given constraint objectives. It is

Table 3: The compared results of the proposed algorithm with the existing algorithms.

	Proposed algorithm	PSO in [20]	HIWO in [21]
N	30	30	30
SLL (dB)	-25	-20	-25
SBL1 (dB)	-26.9	-28.9	-30.9
SBL2 (dB)	-33.6	—	-39.5
Opti. time (s)	2.15	113.39	93

proved that the proposed sequential convex optimization method is effective in the sidelobe and sideband optimization of the main frequency band of the linear array with equal excitation time modulation.

Figure 6 shows the timing of each switch after optimization, where grey indicates that the switch is in the working state and white indicates that the switch is in the inactive state. It can be seen from the results that (1) the working time sequence of the array elements is asymmetric. (2) The working time of the array element in the middle is longer than that in the two sides. (3) The working time efficiency of the array is 90.8%.

4.2. Influence Analysis of Pattern Synthesis Method Based on Array Parameters for Convex Optimization of Discrete Variable Sequences. In order to verify the general applicability of the proposed algorithm, the sidelobe and sideband of the main frequency band are optimized under different radiation angles, different array element numbers, and different array element spacing to verify the effectiveness of the algorithm.

4.2.1. Analysis of the Influence of the Number of Array Elements on the Pattern Synthesis Method for Convex Optimization of Discrete Variable Sequences. In the case of changing the number of array elements (N) (other array parameters remain unchanged with the settings in Table 2), the main frequency sidelobe and sideband are optimized; the comparison results after optimization are given in Table 4.

The results in Table 4 show that (1) when the number of array elements exceeds 30, the sidelobe and sideband constraints reach the specified level (SLL ≤ -25 dB, SBL ≤ -25 dB) after optimization using the proposed algorithm; (2) when the number of array elements is 20, the sidelobe constraint of the main frequency band is too low, which makes the maximum level of the first sideband exceeding the sidelobe level of the main frequency band.

Considering that the algorithm optimizes the sidelobe of the main frequency and sideband when the number of array elements is 20. The sideband level can be adjusted by changing the sidelobe constraint. The relationship between the sidelobe constraint of the main frequency band and the optimized maximum sideband level is shown in Figure 6.

The results of Figure 7 show that for the array with 20 array elements, when the sidelobe level of the main frequency band is below -20 dB (-27 dB~ -20 dB), the optimized SBL1 is between −23.1 dB~ -16.7 dB. When the sidelobe level of the main frequency band is -21 dB, the SBL1 satisfies the constraint condition that is smaller than the sidelobe of the main frequency band and reaches -21.2 dB.

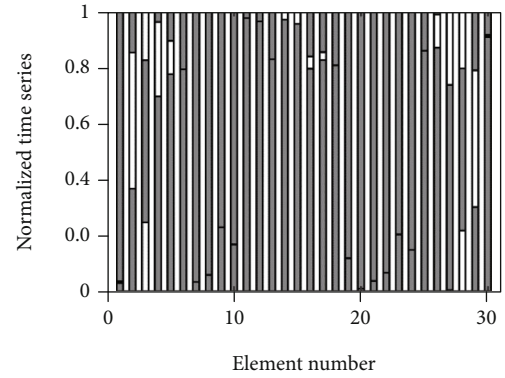

Figure 6: Optimized switching sequence.

Table 4: Optimization effect of different number of array elements.

N	20	30	40	50	60
SLL (dB)	-25	-25	-25	-25	-25
SBL1 (dB)	-18.3	-26.9	-29.8	-31.2	-32.7
SBL2 (dB)	-26.2	-33.6	-38.1	-39.1	-40.8

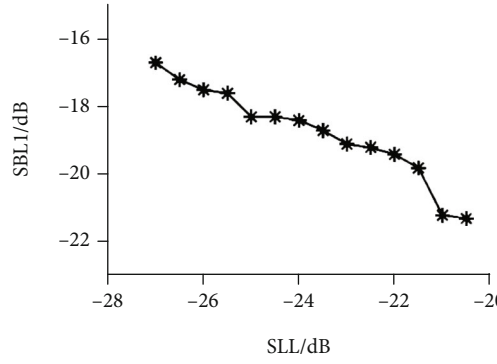

Figure 7: Optimization results of the SBL1 with different SLL for 20 elements array.

4.2.2. Analysis of the Influence of Element Spacing on Pattern Synthesis Method for Convex Optimization of Discrete Variable Sequences. In the case of changing the element spacing (d) (other array parameters remain unchanged with the settings in Table 2), the main frequency sidelobe and sideband are optimized; the comparison results after optimization are given in Table 5.

The results in Table 5 show that (1) when the array element spacing exceeds 0.6λ, the sidelobe and sideband constraints reach the specified level (SLL ≤ -25 dB, SBL ≤ -25 dB) after optimization using the proposed algorithm. (2) When the array element spacing is 0.5λ, the sidelobe constraint of the main frequency band is too low, which makes

Table 5: Optimization effect of different array element spacing.

d	0.5λ	0.6λ	0.7λ	0.8λ	0.9λ
SLL (dB)	-25	-25	-25	-25	-25
SBL1 (dB)	-20.4	-25.3	-26.9	-27.3	-29.7
SBL2 (dB)	-27.3	-30.4	-33.6	-33.7	-35.6

Table 6: Optimization effect under different radiation angles.

θ_0/°	0	10	20	30	40
SLL (dB)	-25	-25	-25	-25	-25
SBL1 (dB)	-26.9	-24.3	-22.3	-21.2	-20.9
SBL2 (dB)	-33.6	-30.7	-27.1	-26.1	-24.2

the maximum level of the first sideband exceeding the sidelobe level of the main frequency band.

Considering the optimization of sidelobe and sideband of the main frequency band under the condition of array element spacing of 0.5λ. The sideband level can be adjusted by changing the sidelobe constraint. When the sidelobe level of the main frequency band is below -20 dB (-27 dB~ -20 dB), the optimized SBL1 is between −22.6 dB~ -18.9 dB. When the sidelobe level of the main frequency band is -21 dB, the SBL1 satisfies the constraint condition that is smaller than the sidelobe of the main frequency band and reaches -21.8 dB.

4.2.3. Analysis of the Influence of Radiation Direction on Pattern Synthesis Method for Convex Optimization of Discrete Variable Sequences. In the case of changing the radiation direction (θ_0) (other array parameters remain unchanged with the settings in Table 2), the main frequency sidelobe and sideband are optimized; the comparison results after optimization are given in Table 6.

The results in Table 6 show that when the radiation direction angle is less than 40°, the sidelobe constraint reaches the specified level (SLL ≤ −25 dB), and the optimization result of the first sideband is $SBL1 \le 20$ dB.

At the same time, when the radiation direction is changed beyond 50°, no matter how to change the sidelobe constraint of the main frequency band, the solution can not be obtained by using the proposed algorithm to optimize the sidelobe and sideband of the main frequency band.

The results of Tables 4–6 show that the optimization effect of the proposed algorithm under different array parameters is obvious (the maximum SBL1 is -16.9 dB, and the maximum SBL2 is -24.2 dB when the sidelobe level of the main frequency band is almost unchanged), which proves the general applicability of the algorithm under different array parameters.

4.3. Sparse Optimization of Equal Excitation Time Array. In order to verify the effectiveness of the method proposed in this paper, set the sparse control coefficient $\gamma \neq 0$. Consider the case of sparsity, the effectiveness of the algorithm is verified by comparing the results of optimized patterns after sparseness with those of the same number of full arrays in the simulation 1. The effect of sparse optimization when the radiation angle changes is further studied.

4.3.1. Validation of Sparse Optimization Algorithm for Equal Excitation Time Array. For the equal excitation time modulated linear array with 30 full array elements before sparse, set the array element interval is half wavelength, and other parameters are the same as Table 2. Set $\lambda_n = 0.6\,(1 \le n \le N)$

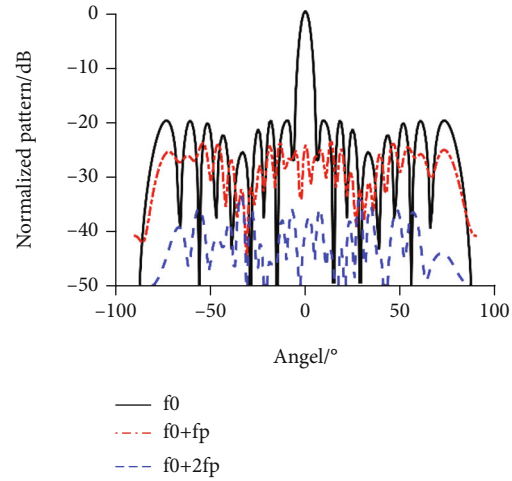

Figure 8: Optimized pattern after sparsity at the central frequency and at front two sidebands of time modulated array.

and $\gamma = 5$. The algorithm can get the sparse array layout results in 3.56 s, and the number of sparse elements is 22. Figure 8 shows the optimized pattern.

The sidelobe level of the main frequency band is controlled at -20 dB; the maximum level of the first sideband and the maximum level of the second sideband are -23.8db and -33.4db, respectively. Compared with the optimization effect of full array of 22 elements without considering sparsity (Table 7 shows comparison results), when the sidelobe level of the main frequency band is almost unchanged, the level of the first sideband decreases by 3.7 dB and 3.2db, respectively, which verifies the effectiveness of the proposed method in sparsity optimization of the equal excitation time modulated linear array elements.

Figure 9 shows the timing of each switch after optimization, where grey indicates that the switch is in the working state, and white indicates that the switch is in the inactive state. The results show that (1) the working time sequence of the array elements is symmetrical. (2) The working time of the array element in the middle is longer than that in the two sides. (3) The working time efficiency of the array is 75.3%.

4.3.2. Determination of Sparse Control Coefficients γ and Comparison Parameter λ. Before applying the proposed algorithm to pattern optimization synthesis, the optimal sparse control coefficient γ and contrast parameter $\lambda_n (1 \le n \le N)$ need to be determined. Define the sparsity degree μ

$$\mu = \frac{\text{Number of working elements after sparsity}}{\text{Number of full array elements}}. \quad (23)$$

Table 7: Overall performances comparison.

Number of elements before sparsity	Number of elements after sparsity	FNBW (°)	Radiation performances of sparse array	Radiation performances of same elements full array
30	22	12	SLL = −20 dB SBL1 = −23.8 dB SBL2 = −33.4 dB	SLL = −20 dB SBL1 = −21.2 dB SBL2 = −30.2 dB
20	16	16	SLL = −20 dB SBL1 = −19.8 dB SBL2 = −25.8 dB	SLL = −20 dB SBL1 = −19.1 dB SBL2 = −25.0 dB
60	38	10	SLL = −20 dB SBL1 = −28.3 dB SBL2 = −33.8 dB	SLL = −20 dB SBL1 = −26.3 dB SBL2 = −33.4 dB

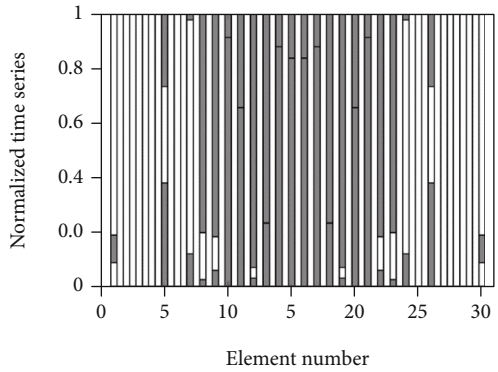

Figure 9: Optimized switching sequence after sparsity.

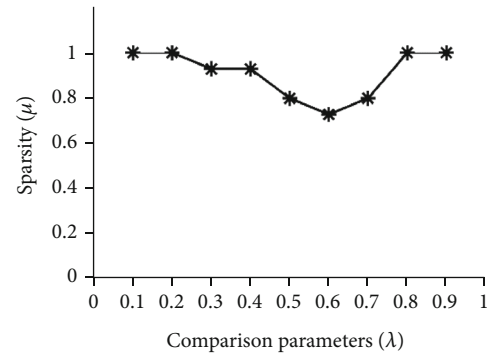

Figure 10: The relationship between contrast parameters λ and sparsity μ.

Considering the equal excitation time modulated linear array with 30 full array elements before sparse, the interval between elements is half wavelength; other parameters are the same as those in Table 2. By changing the parameter of γ and λ, the relationship between the two parameters and the sparsity μ of the array is obtained as follows:

Figure 10 and Table 8 show the change of sparsity μ after the change of comparison parameter λ and sparsity control coefficient γ under the condition of keeping other parameters unchanged. It can be seen that if the comparison parameter λ and the sparse control parameter γ are set too large or too small, the sparsity in the medium will increase. When $\lambda_n = 0.6(1 \le n \le N)$ and $\gamma = 5$, the minimum value of sparsity can be 0.73. Therefore, in the comparative experiment, we use $\lambda_n = 0.6(1 \le n \le N)$ and $\gamma = 5$as the experimental coefficient.

4.3.3. Validation of Sparse Placement Optimization Algorithm with Different Number of Full Array Elements. In order to verify the general effectiveness of the proposed algorithm in the sparse optimization of different full element number array of equal excitation time modulation array, the sparsity optimization algorithm is used to optimize the sidelobe and sideband (under the condition that other conditions unchanged). The comparison results after optimization are shown in Table 7.

The overall comparison of the optimization results in Table 7 shows that the proposed method can achieve good performance in different array elements in the sparsity optimization of equal excitation time modulation array. In each group of comparative experiments, the spared array can obtain lower sideband level under the condition that the sidelobe level of the main frequency band is basically unchanged, which proves the general effectiveness of the algorithm in sparse optimization.

Table 8: The relationship between sparse control coefficient γ and sparsity μ.

γ	0.1	1	5	20	50	100	500
μ	1	1	0.73	0.86	0.86	1	1

4.3.4. Beam Scanning Effect Verification of Sparse Layout Optimization Algorithm. In order to verify the beam scanning effect of the proposed algorithm in the process of sparse optimization, a comparative experiment is set up to verify the beam scanning effect of the sparse algorithm in the sparse optimization by changing the radiation direction (θ_0) of the central frequency under the condition that other conditions remain unchanged.

By using the proposed algorithm, sparse optimization is carried out for the sparse of uniform time modulated linear array with different radiation directions (other array parameters set the same as those in simulation 3.1). The results of sparse optimization for arrays with different radiation

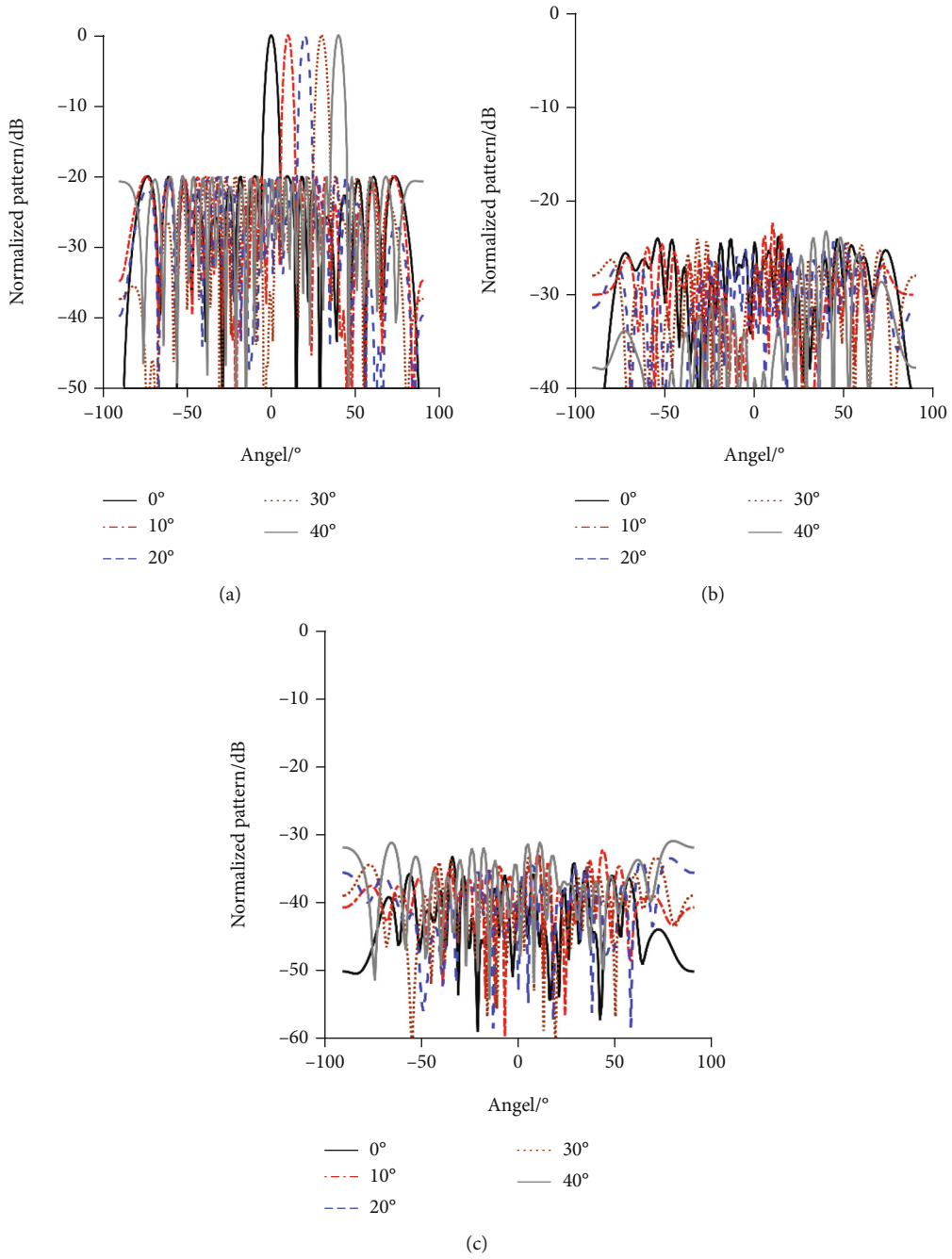

Figure 11: Optimized pattern of different radiation directions after sparsity: (a) at the central frequency; (b) at the first side; (c) at the second side.

directions are shown in Figure 11, and the radiation effect comparison data of different radiation directions after sparse optimization are given in Table 9.

The results in Table 9 and Figure 11 show that the optimization effect of the main frequency band sidelobe and sideband is obvious when using the proposed algorithm in different array radiation directions (the maximum SBL1 is -22.4 dB, and the maximum SBL2 is -29.5 dB when the sidelobe level of the main frequency band is almost unchanged), which verifies the beam scanning effect of the algorithm in the process of sparse optimization.

Table 9: Sparse optimization effect under different radiation angles.

Radiation angles $(\theta_0)/^\circ$	0	10	20	30	40
N after sparsity	22	24	24	26	26
Sparsity (μ)	0.73	0.80	0.86	0.86	0.86
SLL (dB)	-20	-20	-20	-20	-20
SBL1 (dB)	-23.8	-22.4	-24.5	-23.6	-23.2
SBL2 (dB)	-33.4	-32.5	-33.7	-30.5	-30.3

5. Conclusions

In this paper, a sparse optimization method for equal excitation time modulated array based on discrete variables convex optimization is proposed for the first time. The synthesis problem is divided into two parts: In the first part, the discrete variable convex optimization method is used to optimize the number of array elements and the switch-ON duration time to reduce the number of array elements and make the sidelobe of the main frequency band reach the constraint level. In the second part, the iterative convex optimization method is used to optimize the nth switch-ON time instant of the array elements to suppress the sideband. Compared with other methods, the sparse optimization of equal excitation time modulation array is realized effectively, and the optimization time is greatly shortened. The optimization performance of the algorithm is verified when the array parameters are changed to prove the general effectiveness of the algorithm.

Data Availability

The data used to support the findings of this study are available from the corresponding author upon request.

Conflicts of Interest

The authors declare that there is no conflict of interest regarding the publication of this paper.

Acknowledgments

This research was funded by the National Natural Science Foundation of China (Grant no. 61671239) and the Fundamental Research Funds for the Central Universities (Grant no. kfjj20200412 and Grant no. kfjj20200417).

References

[1] P. Rocca, Q. Zhu, E. T. Bekele, S. Yang, and A. Massa, "4-D arrays as enabling technology for cognitive radio systems," *IEEE Transactions on Antennas and Propagation*, vol. 62, no. 3, pp. 1102–1116, 2014.

[2] C. He, H. Yu, X. Liang, J. Geng, and R. Jin, "Sideband radiation level suppression in time-modulated array by nonuniform period modulation," *IEEE Antennas and Wireless Propagation Letters*, vol. 14, pp. 606–609, 2015.

[3] Q. Chen, J.-D. Zhang, W. Wu, and D.-G. Fang, "Single-sideband time-modulated phased array withS-step waveform," *IEEE Antennas and Wireless Propagation Letters*, vol. 19, no. 11, pp. 1867–1871, 2020.

[4] H. Li, Y. Chen, and S. Yang, "Harmonic beamforming in antenna array with time-modulated amplitude-phase weighting technique," *IEEE Transactions on Antennas and Propagation*, vol. 67, no. 10, pp. 6461–6472, 2019.

[5] J. Chen, X. Liang, C. He et al., "Efficiency improvement of time modulated array with reconfigurable power divider/combiner," *IEEE Transactions on Antennas and Propagation*, vol. 65, no. 8, pp. 4027–4037, 2017.

[6] Q. Zhu, S. Yang, L. Zheng, and Z. Nie, "Design of a low sidelobe time modulated linear array with uniform amplitude and sub-sectional optimized time steps," *IEEE Transactions on Antennas and Propagation*, vol. 60, no. 9, pp. 4436–4439, 2012.

[7] Q. Zhu, S. Yang, R. Yao, and Z. Nie, "Gain improvement in time-modulated linear arrays using SPDT switches," *IEEE Antennas & Wireless Propagation Letters*, vol. 11, pp. 994–997, 2012.

[8] C. Sun, S. Yang, Y. Chen, J. Guo, and Z. Nie, "An improved phase modulation technique based on four-dimensional arrays," *IEEE Antennas and Wireless Propagation Letters*, vol. 16, no. 99, pp. 1175–1178, 2017.

[9] S. K. Mandal, H. Singh, A. Mukherjee, and K. Mandal, "A study on variation of side lobe level of optimized uniformly excited time-modulated linear antenna arrays," in *2017 11th European Conference on Antennas and Propagation (EUCAP)*, pp. 3274–3277, Paris, France, 2017.

[10] M. Kumar, B. R. Nenavath, and S. K. Mandal, "Synthesis of uniformly excited time-modulated unequally spaced linear antenna arrays using firefly algorithm (FA)," in *2015 Second International Conference on Advances in Computing and Communication Engineering*, pp. 334–338, Dehradun, India, 2015.

[11] A. Mukherjee, S. K. Mandal, G. K. Mahanti, and R. Ghatak, "Synthesis of simultaneous sum and difference patterns in uniformly excited time-modulated linear arrays using firefly algorithm," in *Proceedings of the 2014 IEEE Students' Technology Symposium*, pp. 143–147, Kharagpur, India, 2014.

[12] A. Mukherjee, S. K. Mandal, G. K. Mahanti, and R. Ghatak, "Simulating optimized time-modulated linear array antennas in CST MWS," in *2013 International Conference on Microwave and Photonics (ICMAP)*, pp. 1–4, Dhanbad, India, 2013.

[13] R. Bhattacharya, S. Saha, and T. K. Bhattacharyya, "Synthesis of thinned uniformly excited time- modulated linear arrays using an improved invasive weed optimization algorithm," in *Proceedings of the 2012 IEEE International Symposium on Antennas and Propagation*, pp. 1-2, Chicago, IL, USA, 2012.

[14] S. K. Mandal, R. Ghatak, and G. K. Mahanti, "Minimization of side lobe level and side band radiation of a uniformly excited time modulated linear antenna array by using Artificial Bee Colony algorithm," in *2011 IEEE Symposium on Industrial Electronics and Applications*, pp. 247–250, Langkawi, Malaysia, 2011.

[15] Y. Liu, Q. H. Liu, and Z. Nie, "Reducing the number of elements in multiple-pattern linear arrays by the extended matrix pencil methods," *IEEE Transactions on Antennas and Propagation*, vol. 62, no. 2, pp. 652–660, 2014.

[16] H. Shen and B. Wang, "An effective method for synthesizing multiple-pattern linear arrays with a reduced number of antenna elements," *IEEE Transactions on Antennas and Propagation*, vol. 65, no. 5, pp. 2358–2366, 2017.

[17] F. Yan, P. Yang, F. Yang, L. Zhou, and M. Gao, "Synthesis of pattern reconfigurable sparse arrays with multiple measurement vectors FOCUSS method," *IEEE Transactions on Antennas and Propagation*, vol. 65, no. 2, pp. 602–611, 2017.

[18] P. You, Y. Liu, S.-L. Chen, K. Da Xu, W. Li, and Q. H. Liu, "Synthesis of unequally spaced linear antenna arrays with minimum element spacing constraint by alternating convex optimization," *IEEE Antennas and Wireless Propagation Letters*, vol. 16, pp. 3126–3130, 2017.

[19] F. Yang, S. Yang, Y. Chen, S. Qu, and J. Hu, "Efficient pencil beam synthesis in 4-D antenna arrays using an iterative convex optimization algorithm," *IEEE Transactions on Antennas and Propagation*, vol. 67, no. 11, pp. 6847–6858, 2019.

[20] L. Poli, P. Rocca, L. Manica, and A. Massa, "Handling sideband radiations in time-modulated arrays through particle swarm optimization," *IEEE Transactions on Antennas and Propagation*, vol. 58, no. 4, pp. 1408–1411, 2010.

[21] Y. Liu and Y. Zhang, "A novel hybrid evolutionary algorithm for pattern synthesis in time-modulated antenna arrays," in *2019 IEEE 9th International Conference on Electronics Information and Emergency Communication (ICEIEC)*, pp. 608–610, Beijing, China, 2019.